Journal of Sedimentary Environments
https://doi.org/10.1007/s43217-024-00194-6

RESEARCH

Petrography and mineralogy of the Wessex Basin: palaeoclimate and palaeoenvironments of Lower Cretaceous in southern England

Oladapo O. Akinlotan[1] · Ogechukwu A. Moghalu[2] · Okwudiri A. Anyiam[2]

Received: 25 January 2024 / Revised: 24 June 2024 / Accepted: 28 July 2024

Abstract
The Wessex Basin has been the focus of extensive studies on vertebrate palaeontology and is globally famous for dinosaur remains. Nevertheless, detailed mineralogical and petrographic studies have however been recently focused on the adjacent Weald Basin. An integrated approach comprising optical microscopy, scanning electron microscopy, energy dispersive spectrometry and Quantitative Evaluation of Minerals by Scanning Electron Microscopy were used to study the sandstones, mudstones and ironstones within the basin. Feldspathic and quartz wackes, subarkose and quartz arenites are the sandstone types identified. The results revealed a high quartz content with little feldspar concentration that is largely of K-feldspars and Na-rich plagioclase. Heavy minerals include rutile, tourmaline, zircon, apatite, ilmenite, olivine, amphibole, pyroxene, magnetite, monazite, epidote, and garnet. Compositionally, the sandstones are sub-mature to super-mature while they range from immature to submature texturally. The presence of apatite within the sandstones indicates that the sediments have not been affected by any significant post-depositional diagenetic modifications at the site of deposition. The significant concentrations of heavy mineral suite of garnet and rutile indicate metamorphic origin for the sediments within the Wessex Basin with a possibility of mixture of metamorphic and igneous materials at the source areas. The high monocrystalline quartz content, with subordinate K-feldspars and heavy mineral concentration indicates that they have been recycled from older sedimentary materials within the source massifs. The textural maturity of the sandstones reflects moist and warm climatic conditions that favoured a high degree of weathering and transport processes that have removed most of the unstable grains.

Keywords Lower Cretaceous · English wealden · Wessex basin · Palaeoenvironments · Petrography

1 Introduction

The mineralogical composition of clastic sedimentary rocks is routinely used to infer their tectonic settings, provenance, palaeoclimatic and weathering conditions, transport system, post-depositional and/or diagenetic transformation (e.g. Akinlotan et al., 2021a; Akinlotan, 2015, 2017a, 2017b; Dickinson, 1985; Dickinson & Suczek, 1979; Jenchen, 2018; Mohammedyasin & Wudie, 2019). Quartz and feldspar are the major constituents of sedimentary rocks while rock fragments and heavy minerals do occur as secondary minerals although some sandstones may contain glauconite, iron, etc. (e.g. Dickinson, 1985; Dickinson & Suczek, 1979). The amount of quartz in a sedimentary facies can be very useful for understanding provenance, climate pattern, transport system, and tectonic settings in the source areas (e.g. Dickinson, 1985; Dickinson & Suczek, 1979). Quartz arenites are considered matured if they are rich in quartz (more than 95% of grain framework) and devoid of feldspars (Dickinson, 1985; Folk, 1980). As result of their high composition of quartz grains, quartz arenites can indicate tectonic settings at the source areas, help to distinguish between igneous and metamorphic provenances, describe intensive weathering pattern, indicate tropical climates, reveal long sediment transport or sediment recycling (Basu, 1985; Dickinson, 1985; Dickinson & Suczek, 1979). On the other hand, the concentration of feldspar in sandstones can reveal palaeoclimatic and palaeoweathering conditions at the source areas (Basu, 1985; Dickinson, 1985; Dickinson

Communicated by M. V. Alves Martins

✉ Oladapo O. Akinlotan
oladapo.akinlotan@aru.ac.uk

[1] Anglia Ruskin University, Bishop Hall Lane, Chelmsford CM1 1SQ, UK

[2] Department of Geology, University of Nigeria, Nsukka Road, Nsukka 410001, Nigeria

Published online: 07 August 2024

& Suczek, 1979). Since the breakdown of feldspar leads to the formation of kaolinite, the presence or absence of feldspar can be useful for understanding clay mineral formation (Akinlotan et al., 2022; De Segonzac, 1970; Eberl, 1984).

The Wessex Basin in central-southern England (Fig. 1) is one of the Lower Cretaceous basins in southern England with fluvial, lacustrine and lagoonal facies (Akinlotan, 2016, 2018, 2019; Allen, 1975, 1981; Stewart, 1978). The basin has been the focus of extensive studies on vertebrate palaeontology particularly dinosaurs for which the basin is globally famous (e.g. Radley et al., 1998a; Sweetman, 2006). Major dinosaur fossils have been described (e.g. Insole & Hutt, 1994; Pereda-Suberbiola, 1993; Radley et al., 1998a). It is worth mentioning that Allen's extensive mineralogical work (e.g. Allen & Krumbein, 1962; Allen & Wimbledon, 1991; Allen, 1948, 1959, 1967, 1972a, 1972b, 1975, 1981, 1989, 1991; Allen et al., 1973) have been crucial in understanding Wealden palaeogeography in the Wessex Basin and the adjacent Weald basin. In addition to these studies, there have been various sedimentological studies on the Wessex Basin (e.g. Daley & Stewart, 1979; Osborne White, 1921; Penn et al., 2020; Radley & Barker, 1998b; Stewart, 1981b). While diagenetic evolution of the Wessex Basin sandstones has been described recently (Akinlotan & Hatter, 2022), detailed mineralogical and petrographic studies have, however, been recently focused on the adjacent Weald Basin (e.g. Akinlotan et al., 2021a, 2022; Akinlotan, 2017b, 2018; Kemp et al., 2012). The aim of this study is to use the mineralogical compositions of the facies to understand their depositional and paleoenvironmental conditions by examining their tectonic settings, provenance, weathering conditions, transport system, post-depositional and/or diagenetic transformation. This current study presents comprehensive petrographic and mineralogical datasets for the Wessex Basin to validate previous interpretations made from sedimentology and palaeontology datasets. This is the only study as far as we know that have used an integrated approach (optical microscopy, scanning electron microscopy, energy dispersive spectrometry and Quantitative Evaluation of Minerals by Scanning Electron Microscopy) in a single study to conduct mineralogical and petrographic descriptions of the sediments within the Wessex Basin. The results of this study would be very useful to support interpretations from field and fossil proxies within the Wessex Basin and other basins elsewhere.

2 Geological settings

The Wessex Basin (Fig. 1) has been described in detail (e.g. Akinlotan & Rogers, 2021; Daley & Stewart, 1979; Stewart, 1978; Stewart et al., 1991) and briefly summarised here. The non-marine lowermost Cretaceous sediments exposed in coastal areas of Dorset (Fig. 1) and Isle of Wight (Fig. 1) and generally equate to the Wessex Basin and range from the Berriasian to earliest Aptian (Stewart, 1978). The basin developed as one of the rifted basins associated with the Permo-Triassic rifting episodes in southern England (Lake & Karner, 1987; Stoneley, 1982). The basin is normally divided into two formations (Fig. 2): Wessex and Vectis which were previously known as Wealden Marls and Wealden Shales respectively (Stewart, 1978). All these sediments within the basin were sourced from adjacent massifs: mainly Cornubia and Armorica (Allen, 1975, 1981) and were deposited in non-marine environments including fluvial and lagoonal settings (Stewart, 1981a, 1981b, 1983).

In terms of facies and lithology, the Wessex Formation is made up of multi-coloured mudstones, sandstones and some sideritic ironstones and these are exposed in coastal sections at Swanage Bay and Mupe Bay (Fig. 1), Punfield Cove and Bacon Hole (Hopson et al., 2008). The Vectis Formation has varied lithology consisting of dark grey siltstones and mudstones with minor sandstone, shelly limestone, clay ironstone and sideritic ironstone. The formation has key outcrops at Brighstone Bay, Sandown Bay and Compton Bay in the Isle of Wight (Fig. 1). Three members based on three

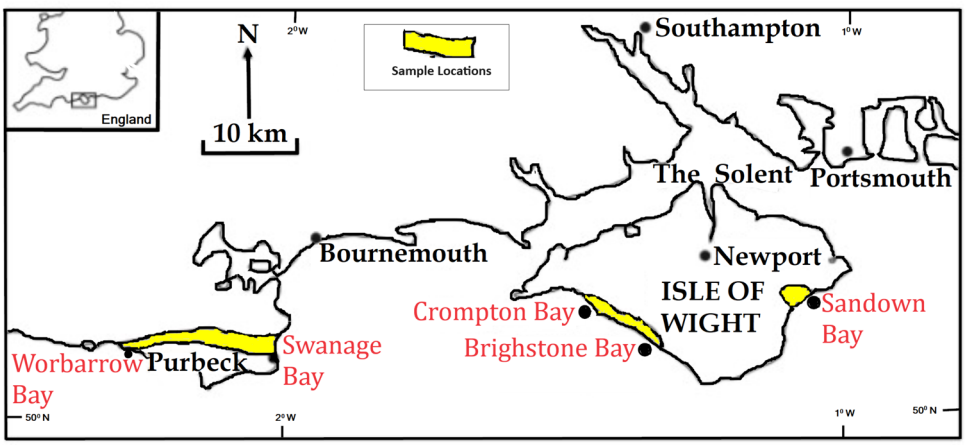

Fig. 1 The Wealden outcrops in Dorset and Isle of Wight southern England and the study sample locations, Yaverland is part of Sandown Bay, after Radley and Barker (1998a)

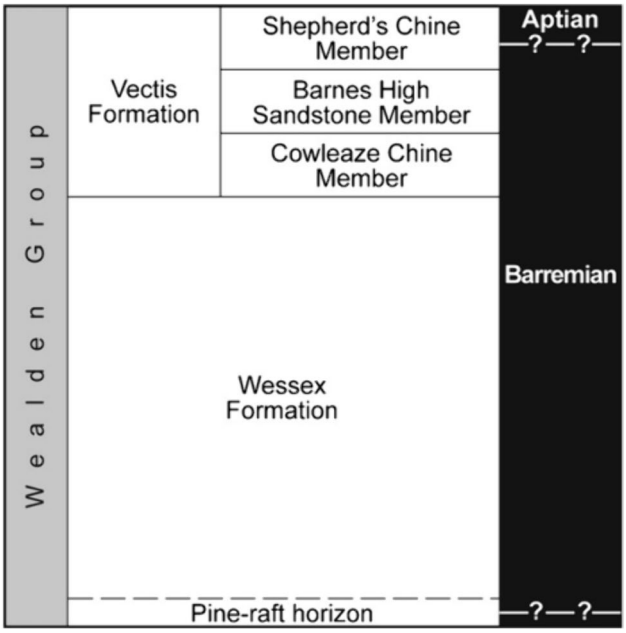

Fig. 2 The Lower Cretaceous stratigraphy at Isle of Wight after Radley and Allen (2012b)

distinct facies from the Vectis Formation has been described (Daley & Stewart, 1979; Stewart, 1981a): the Cowleaze Chine Member, the Barnes High Member and the Shepherd's Chine Member (Fig. 2). The Cowleaze Chine Member (oldest) consists of bioturbated dark grey mudstones and pale grey silt/fine-grained sandstone. The Barnes High Sandstone Member is a medium-grained yellow to grey sandstone with poorly preserved sedimentary structures. The Shepherd's Chine Member (youngest) consists of light to dark grey fine-grained sandstones, siltstones and mudstones with bioturbated and fossiliferous grey mudstones (Fig. 2).

3 Methodology

3.1 Field studies

Field studies were carried out in five type sections of the Wealden facies within the Wessex Basin in Dorset and Isle of Wight (Fig. 1) and a total number of seventy-four samples were collected (Fig. 3). A summary of lithological and sedimentological details is briefly described (Fig. 4). The section at Swanage exposes about 350 m of varicoloured mudstones, fine to coarse-grained sandstones, ironstones and lignitic plant debris beds. The sandstone bodies display through cross-bedding, syn-sedimentary deformation, lateral accretion surfaces (Radley & Allen, 2012b). The sampled section comprises mainly mudstone and sandstone from the Wessex Formation (Fig. 4). The mudstone is varicoloured while the sandstone is fine to coarse-grained. The sandstone displays trough cross-bedding. The Worbarrow Bay exposes about 418 m thick of Wessex Formation: varicoloured mudstones, coarse sandstones, ironstones and occasional plant debris beds. The sandstones exhibit cross-beddings and are medium-grained sandstones (Radley & Allen, 2012b; Stewart, 1978). The sampled section consists of multiple facies within the Wessex Formation. These are varicoloured mudstones, coarse sandstones, ironstones and shales. The sandstone bodies are cross-bedded, have fining-upward units, with flat-bedded lower portions (Fig. 4). At Crompton Bay, the Wessex Formation is about 125–150 m thick and represented by oxidized, varicoloured and predominantly red mudstones with rootlet traces (Radley & Allen, 2012b). The Vectis Formation is about 21 m thick and are represented by grey, shelly, shaly mudstones (some fossiliferous), bioturbated silty mudstones and thin sandstones. The sandstones display cross-bedding, wavy flaser bedding, mega ripples, large-scale trough and planar cross-beds and mudclasts (Radley & Allen, 2012b). At Crompton Bay section, both the Wessex and Vectis formation are exposed and sampled (Fig. 4). The Wessex Formation is represented by varicoloured and red mudstones. The Vectis Formation consist of shaly mudstones, thin sandstones, shales and ironstone. The sandstone displays wavy flaser bedding, large-scale trough and planar cross-beds. At Brighstone, the Wessex Formation is about 180 m thick while Vectis Formation is about 55 m thick. The Wessex Formation exposes varicoloured mudstones and layers of reworked ironstone nodules. The Vectis Formation is represented by grey mudstones (Radley & Allen, 2012b). The sampled section at Brighstone represents varicoloured mudstones with rootlet traces within the Vectis Formation (Fig. 4). The Yaverland section exposes both the Wessex Formation (50 m thick) and Vectis Formation (45 m thick). The section consists of shaly, blocky grey, grey-coloured mudstones, interbedded mudstones, and cross-laminated, lenticular and bioturbated fine sandstones with flaser-beddings and clay-ironstones (Radley & Allen, 2012b). The sampled section consists of mainly mudstones and minor shale and sandstone from the Vectis Formation. The mudstone is blocky and grey-coloured while the sandstone is coarse-grained with cross- and flaser beddings (Fig. 4).

3.2 Laboratory analyses

A total number of seventy-four (74) representative surface samples which were collected from the field locations were all subjected to Quantitative Evaluation of Minerals by Scanning Electron Microscopy (QEMSCAN®) analysis. QEMSCAN® technique was used to determine the bulk mineralogy of the sandstones using a QUANTA 650F machine based on the technique previously described (Akinlotan &

No	Sample Code	Location & Formation	Grid Reference	Lithology	Analyses		
					QEMSCAN	Thin section	SEM +EDX
1	YA8	YAVERLAND (Vectis Formation)	SZ 611 850	Yellowish sandstone	✓	✓	✓
2	YA7			Darkish mudstone	✓		
3	YA6			Shale	✓		
4	YA5			Greyish mudstone	✓		
5	YA4			Greyish mudstone	✓		
6	YA3			Greyish mudstone	✓		
7	YA2			Greyish mudstone	✓		
8	YA1			Brownish mudstone	✓		
9	BB5	BRIGHSTON E BAY (Vectis Formation)	SZ 425 805	Brownish mudstone	✓		
10	BB4			Greyish mudstone	✓		
11	BB3			Greyish mudstone	✓		
12	BB2			Greyish mudstone	✓	✓	✓
13	BB1			Greyish-brownish mudstone	✓		
14	CB2-16	COMPTON BAY-RIGHT (Vectis Formation)	SZ 363 847	Darkish mudstone	✓		
15	CB2-15			Mudstone	✓		
16	CB2-14			Mudstone	✓		
17	CB2-13			Shale	✓		
18	CB2-12			Ironstone	✓	✓	✓
19	CB2-11			Shale	✓		
20	CB2-10			Iron-cemented mudstone	✓	✓	✓
21	CB2-9			Greyish mudstone	✓		
22	CB2-8			Greyish mudstone	✓		
23	CB2-7			Greyish mudstone	✓		
24	CB2-6			Shale	✓		
25	CB2-5			Light-greyish mudstone	✓		
26	CB2-4			Greyish mudstone	✓		
27	CB2-3			Darkish Grey mudstone	✓		
28	CB2-2			Greyish mudstone	✓		
29	CB2-1			Greyish mudstone	✓		
30	CB1-10	COMPTON BAY – LEFT (Wessex Formation)	SZ 363 847	Greyish mudstone	✓		
31	CB1-9			Greyish mudstone	✓		
32	CB1-8			Dark-greyish mudstone	✓		
33	CB1-7			Greyish mudstone	✓		
34	CB1-6			Greyish mudstone	✓		
35	CB1-5			Greyish mudstone	✓		
36	CB1-4			Light-greyish mudstone	✓		
37	CB1-3			Greyish mudstone	✓		
38	CB1-2			Brownish fine-grained sandstone	✓		✓
39	CB1-1			Greyish mudstone	✓		
40	WB17	WORBARROW (Wessex Formation)	SY 864 799	Iron-cemented sandstone	✓		
41	WB16			Iron-cemented mudstone	✓	✓	✓
42	WB15B			Ironstone	✓	✓	✓
43	WB15A			Iron-cemented sandstone	✓		
44	WB14			Greyish sandstone	✓		
45	WB13B			Greyish mottled mudstone	✓		
46	WB13A			Iron-cemented sandstone	✓		
47	WB12			Ironstone	✓	✓	✓
48	WB11			Shale	✓		
49	WB10			Ironstone	✓		
50	WB9			Greyish mudstone	✓		
51	WB8			Greyish mottled mudstone	✓		
52	WB7			Brownish mudstone	✓		
53	WB6B			Greyish mudstone	✓		
54	WB6A			Greyish mudstone	✓		
55	WB5B			Red sandstone	✓		
56	WB5A			Greyish mudstone	✓		
57	WB4			Greyish mudstone	✓		
58	WB3B			Red coarse sandstone	✓		✓
59	WB3A			Greyish mudstone	✓		
60	WB2B			Reddish-brown sandstone	✓		
61	WB2A			Greyish mudstone	✓		
62	WB1B			Darkish shale	✓		
63	WB1A			Greyish mottled mudstone	✓		
64	SW9	SWANAGE BAY (Wessex Formation)	SZ 038 808	Greyish mudstone	✓		
65	SW8			Greyish mudstone	✓		
66	SW7			Greyish mudstone	✓		
67	SW6B			Greyish mudstone	✓		
68	SW6A			Greyish mudstone	✓		
69	SW5			Greyish fine-grained sandstone	✓		
70	SW4			Greyish fine-grained sandstone	✓		
71	SW3			Greyish fine-grained sandstone	✓	✓	✓
72	SW2B			Greyish mudstone	✓		

Fig. 3 The stratigraphy and lithology of the samples used for this study (Wessex Formation). QEMSCAN®: Quantitative Evaluation of Minerals by Scanning Electron Microscopy; SEM: Scanning Electron Microscopy; EDS: Energy Dispersive Spectrometry

Rogers, 2021; Akinlotan et al., 2021b; Knappett et al., 2011; Zhang et al., 2015). For QEMSCAN® technique, samples were either prepared into thin section or made into polished resin blocks using a maximum sample surface area of 7.29cm^2 and 5.4cm^2, respectively.

Out of the seventy-four field samples, ten (10) representative samples (4 sandstones, 3 ironstones and 3 mudstones) that can show petrographic features were selected for optical petrographic analyses (Fig. 3). Petrographic studies involved mineral identification, point counting of framework grains and accessory minerals, as well as matrix and cement estimation, which allowed for sandstone classification. The classification scheme of Pettijohn et al. (1987) was used. The optical microscopy techniques used in the study such as mineral identification, grain size, grain counting, sorting, etc. were based on previously described techniques (e.g. Akinlotan et al., 2021a; Akinlotan, 2017b; Jenchen, 2018; Mohammedyasin & Wudie, 2019). A Zeiss AX10 transmitted light microscope was used to acquire petrographic images which were used to support petrographic descriptions.

The same samples used for petrographic analyses were also subjected to scanning electron microscopy (SEM) from which selected minerals were subjected to energy dispersive spectrometry (EDS) analyses. A QUANTA 650F machine was used for SEM analysis with a BSE detector and a secondary electron detector. Bruker EDS detectors were used to acquire EDS data and analysed using Bruker's ESpirit software. Identification of minerals in thin sections and SEM/EDS was aided using relevant sources (e.g. Adams et al., 1984; Fang et al., 2017; Kim et al., 2004; Romero-Guerrero et al., 2018; Ulmer-Scholle et al., 2014). The technique used in this study is based on previously described technique (e.g. Akinlotan et al., 2021a; Nie & Peng, 2014; Pirrie et al., 2009). All the analyses described above were carried out at CGG Robertson, North Wales, United Kingdom.

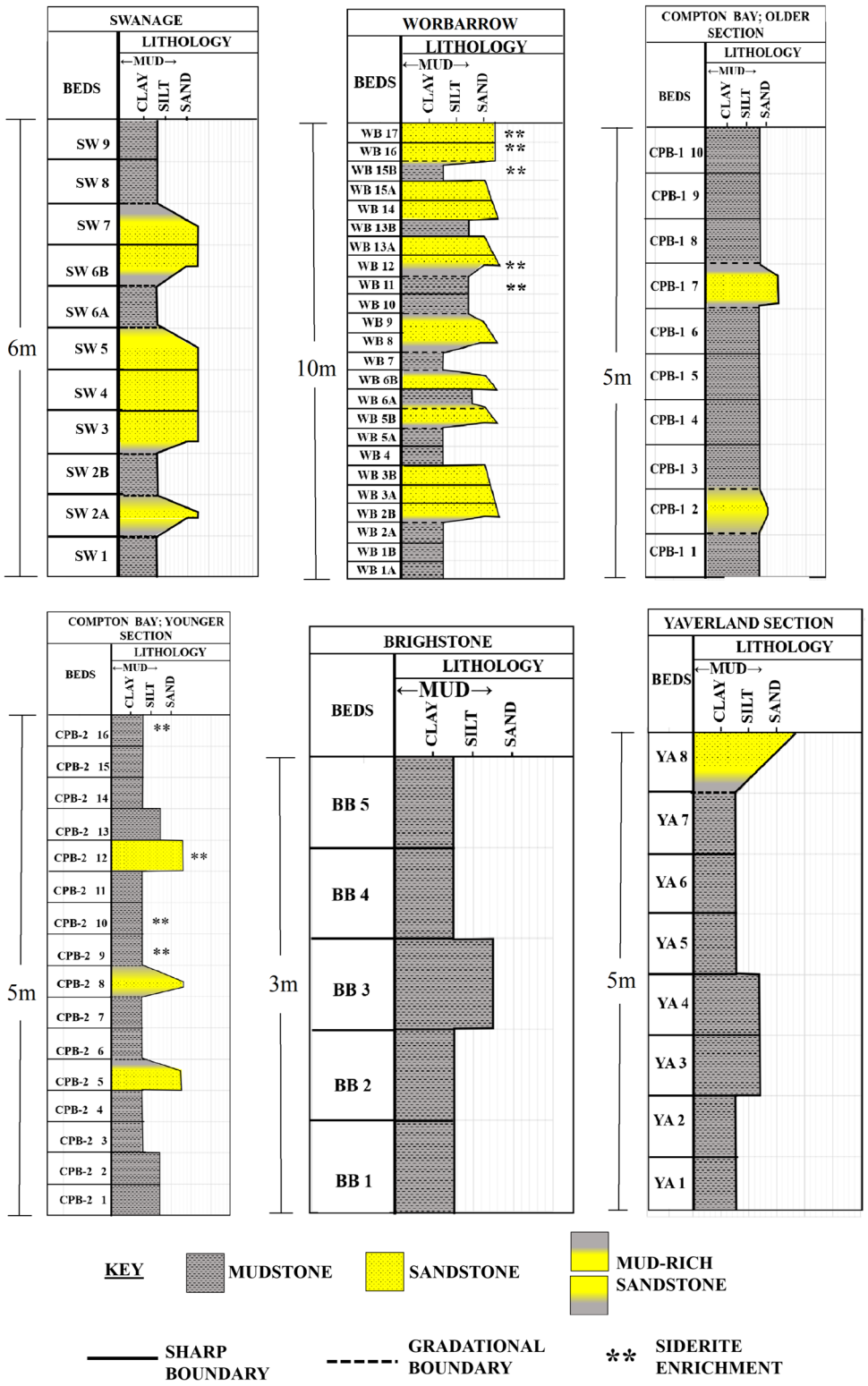

Fig. 4 Composite logs showing lithologies and key sedimentary characteristics of the studied sections

Table 1 Modal composition in percentages of the selected samples from the Wessex Basin based on optical microscopy

Mineral	Description	SW-3	WB-12	WB-15B	WB-16	CPB-1-2	CPB-2-10	CPB-2-12	BB-2
Quartz	Monocrystalline	81.0	57.5	67.0	10.0	63.0	70	52	94
	Polycrystalline	3.0	1.0	1.0	-	3.0	-	-	2
Feldspar	K-feldspar	8.0	1.0	2.5	1.0	3.5	-	2	2
	Plagioclase	0.5	-	-	-	2.0	-	-	-
Lithic fragment	Sedimentary	2.0	1.0	-	-		1	-	-
	Igneous	3.0	-	0.5	-	2.5	-	-	-
	Metamorphic	-	-	-	-	-	-	-	-
Heavy mineral	Rutile	-	-	-	-	-	-	-	-
	Garnet	0.5	-		-	0.1	1	1	-
	Tourmaline	0.5	-	1.0	0.5	0.2	1	-	-
	Zircon	-	-	-	-	0.2	1	-	-
	Apatite	-	-	-	-	0.2	2	-	-
	Ilmenite	-	-	-	-	0.3	2	-	-
Matrix		1.5	12.0	17.0	40.0	20.0	2	45	-
Cement	Siderite	-	27.5	11.0	15.0	5.0	20	-	2
	Calcite	-	-	-	33.5	-	-	-	-

Sandstone | Ironstone | Mudstone

CPB-2 (1) is not included because it is composed of > 90% of matrix and cement. The colour represents the lithology of the samples

4 Results

4.1 Optical microscopy

Optical microscopy of rock samples from the Wessex Formation reveals generally muddy to sandy rocks (Figs. 6, 7; Table 1). The sands are moderately sorted. Minerals identified in the samples include quartz, feldspar (K-feldspar and plagioclase), garnet, tourmaline, ilmenite, and apatite and zircon (Figs. 6a, b, 7a–d, Table 1). The framework composition is mainly grain-supported. The shape of the grains is generally angular. Compaction is demonstrated by a loose packing dominated by non-grain contacts (long, floating and tangential) although with minor concave–convex contacts are observed in samples from Compton Bay (Fig. 6). The quartz grains are predominantly monocrystalline, with minor occurrences of polycrystalline quartz (Fig. 5). Feldspar content has more K-feldspar than plagioclase (Fig. 5). Lithic fragments of volcanic and metasedimentary origin are also evident (Figs. 5a, b; e–f, 6). Cementation is mostly by formation of an iron-rich mineral, siderite (Fig. 5c–e; Table 1), which coats the grains. In some cases, intergranular pore spaces within the grain framework have been replaced by siderite cement. However, sample WB-16 has more calcite cement than iron-rich cement (Fig. 5f, g; Table 1). Within the Vectis Formation, samples CPB-2–10 and BB-2 are mudstones (Figs. 6c, d and 7a, b), while samples CPB-2–12 and YA-8 are sandstones (Figs. 6c–f, 7c, d). The sandstones have moderate sorting like the sandstones in the Wessex Formation. Grain shape ranges from angular to sub-rounded (Figs. 6c–f, 7c, d). Compaction is demonstrated by moderate packing with most grains in a mix of point, long and tangential contact, with rare grains displaying concave-convex or non-grain contact. Siderite concretions (ooids) are observed in sample CPB-2–12 (Fig. 6e, f).

4.2 SEM/EDS

Examination of SEM/EDS images of samples from the Wessex Basin reveals the presence of framework (quartz) and accessory minerals such as rutile, apatite, and ilmenite (Fig. 8a, c, e, g, h, j). Quartz is recognized by spikes in Si and O on the EDS spectra (Fig. 9). Rutile is detected in one of the samples at Worbarrow Bay (Fig. 8c), with higher concentrations of Ti and O, compared to other elements (Fig. 9c). A concentration of apatite crystals is observed in a sample from the older section of the Compton Bay (Fig. 8f). Its EDS spectra shows spikes in Ca, P, and O (Fig. 9f). Ilmenite is detected in the sample from Brighstone

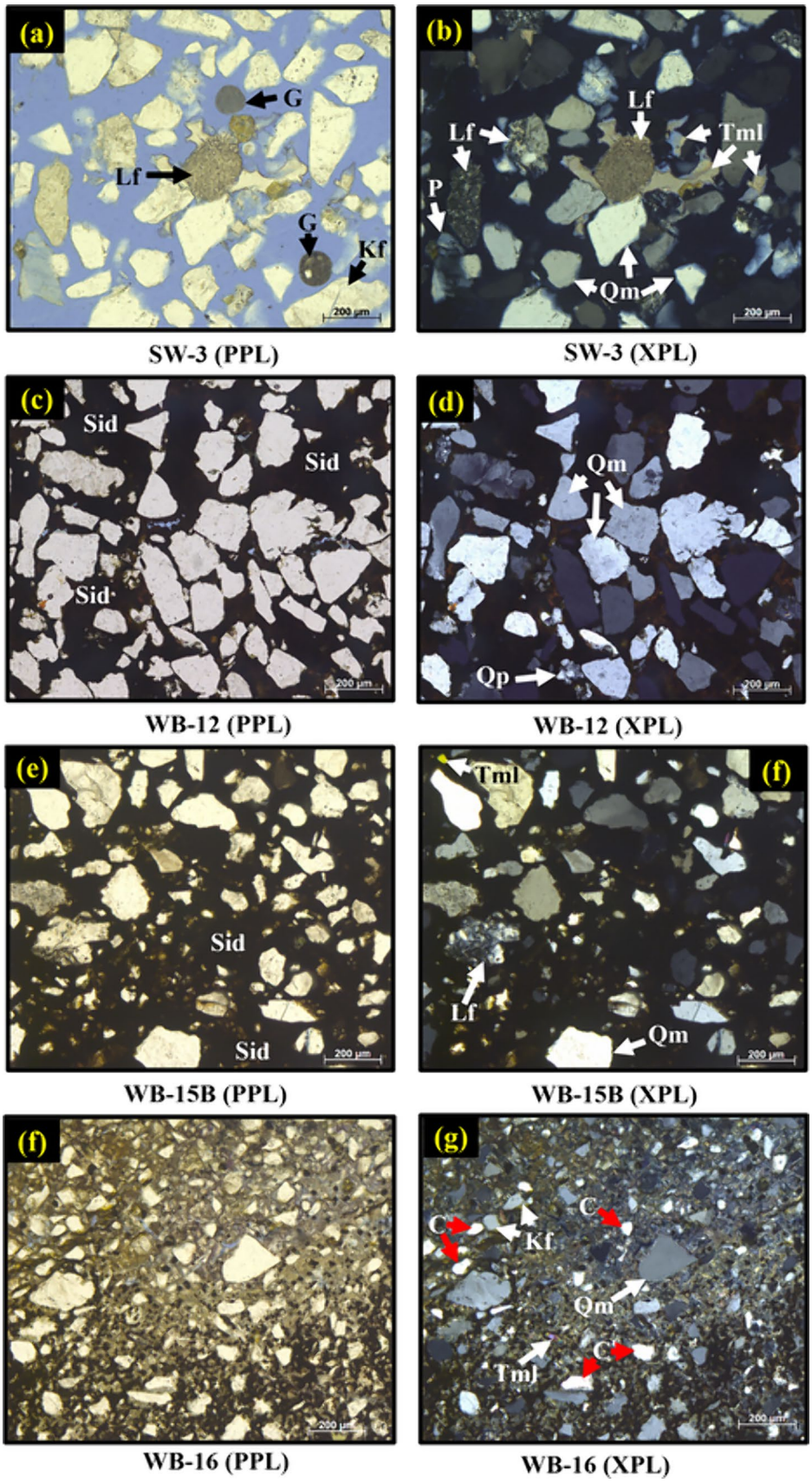

Fig. 5 Thin section photos of selected samples from the Wessex Formation under plane-polarised light (PPL) and cross-polarised light (XPL). Monocrystalline quartz (Qm), polycrystalline quartz (Qp), K-feldspar (Kf), plagioclase (P), lithic fragment (Lf), garnet (G), tourmaline (Tml), calcite (C) and siderite (Sid). Samples' locations: Swanage (SW) and Worbarrow (WB)

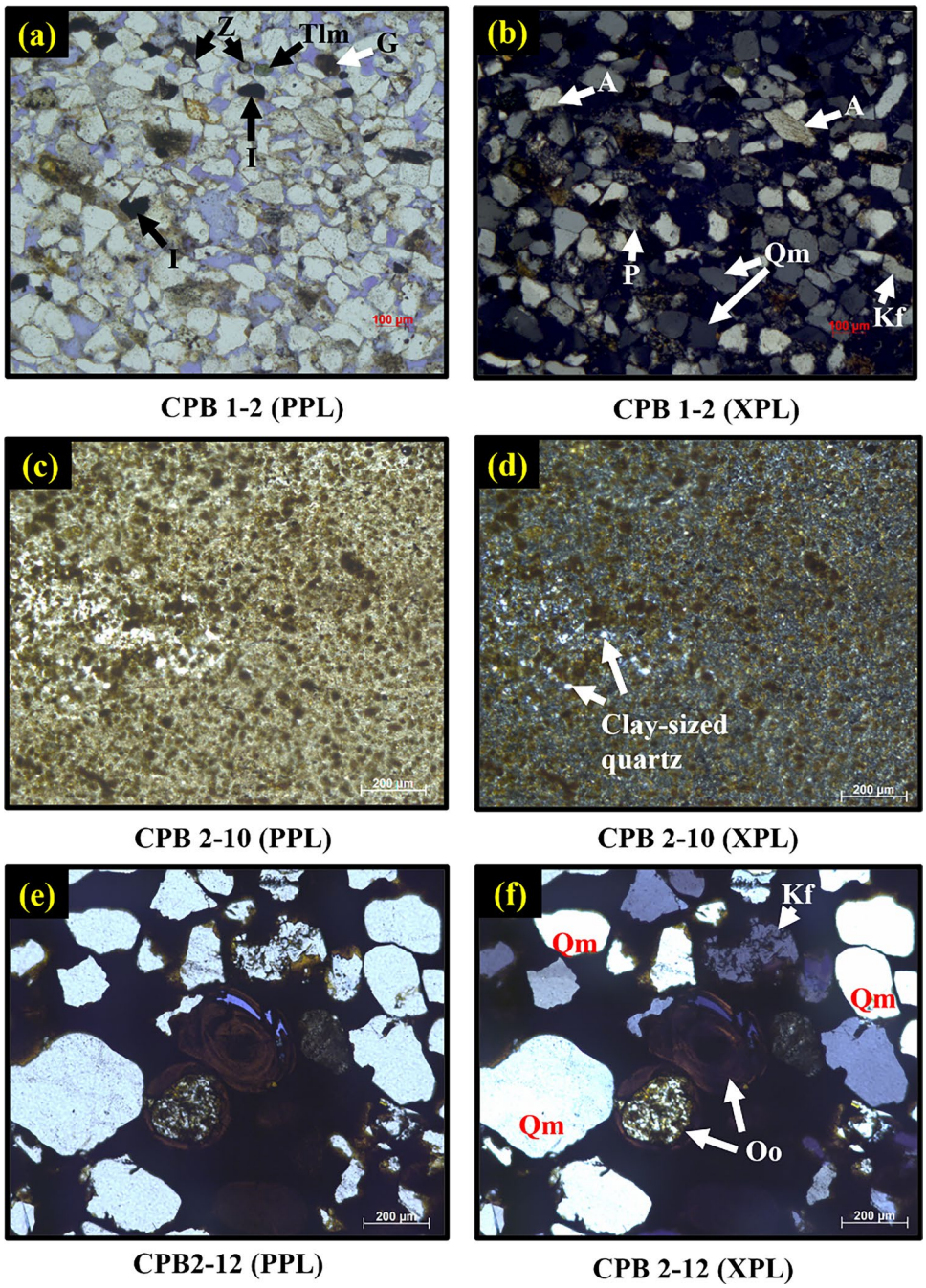

Fig. 6 Thin section photos of selected samples from the Compton Bay section (across the boundary between the Wessex and Vectis formations) under plane-polarised light (PPL) and cross-polarised light (XPL). Monocrystalline quartz (Qm), K-feldspar (Kf), plagioclase (P), apatite (A), ilmenite (I), garnet (G), tourmaline (Tml), zircon (Z) and ooids (Oo). Samples' locations: Compton Bay, older section (CPB-1) and Compton Bay, younger section (CPB-2)

Bay (Fig. 8i). Its chemical composition, which is made up of Fe, Ti and O, is reflected in its EDS spectra (Fig. 9i), as these elements have the highest concentrations. Siderite and ferroan calcite are also identified (Fig. 8b, d, and h). The EDS spectra of siderite shows Fe, C and O, having the highest concentrations (Fig. 9b), while ferroan calcite, has Fe, Ca, and O as the elements with the highest concentrations (Fig. 9d).

4.3 QEMSCAN®

The mineralogical compositions based on QEMSCAN® analyses show an array of minerals from framework minerals such as quartz, K-feldspar and plagioclase, clay minerals and micas, and cement minerals (Table 2). Examination of the QEMSCAN® datasets reveal quartz as the dominant mineral in all the samples (Table 2) except WB-16, which is dominated by calcite. Feldspars are also present in relatively considerable quantities in the samples SW-3, CPB-1–2, CPB-2–12 and BB-2. The framework minerals (quartz

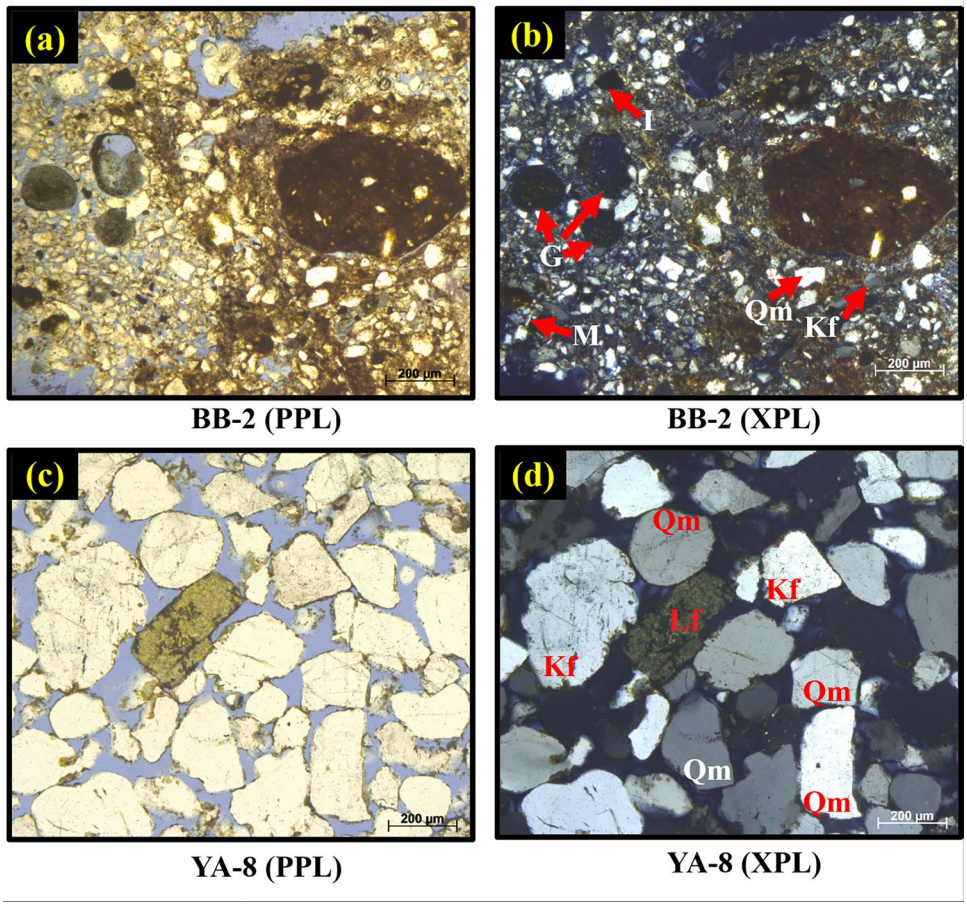

Fig. 7 Thin section photos of selected sandstone (YA-8) and mudstone (BB-2) from the Vectis Formation under plane- polarised light (PPL) and cross-polarised light (XPL). Monocrystalline quartz (Qm), K-feldspar (Kf), muscovite (M), lithic fragment (Lf), ilmenite (I), and garnet (G). Samples' locations: Brighstone (BB) and Yaverland (YA)

and feldspar) constitute about ca. 14 to 98% of the bulk mineralogy (Table 2 and Appendix 1). Total clay minerals (kaolinite, illite, chlorite, smectite and glauconite) and mica (biotite and muscovite) range from ca. 0.8 to 44% while the proportion of cement ranges from ca. 0.2 to 76% and is dominated by siderite and calcite (Table 2 and Appendix 1). Rutile and apatite are the most predominant heavy minerals in the Wessex Formation. Other significantly enriched heavy minerals in decreasing order are tourmaline, ilmenite, garnet olivine, zircon, pyroxene and epidote. Apatite is the dominant heavy mineral within the Vectis Formation while rutile, tourmaline, ilmenite, and olivine are other important heavy minerals (Table 2 and Appendix 1).

It is important to mention that there are some differences in the data reported in the current study (e.g. high apatite concentration) compared to previous data (e.g. Allen, 1948) and possible explanations are provided here. Previous studies (e.g. Allen, 1948, 1972b) did not use QEMSCAN® method but used conventional petrographic method, whereas current study used a combination of conventional petrographic and QEMSCAN® methods. In addition to this, different samples have been analysed due to different study locations for the previous and current studies. For example, Allen (1948) sampled Ashdown Pebble Bed and the Top Ashdown Sandstone within the Ashdown Formation in the Weald Basin while current study sampled locations in the adjacent Wessex Basin for current investigation. Despite the differences in datasets, the interpretations made from the current study align with interpretations from previous studies.

5 Interpretation

5.1 Rock classification

Mineralogy based on optical microscopy (Figs. 7, 8, 9) shows that the selected samples from the Wessex Basin are mainly sandstones, mudstones and ironstones (Tables 1 and 2). The sandstones can be divided into two petrofacies based on their mineralogy (Pettijohn et al., 1987). The first petrofacies are the wackes WB-15B and CPB-1–2 (Fig. 10). Sample WB-15B is a quartz wacke (Fig. 10). This sandstone has a clay mineral + mica content that is > 15% of the bulk mineralogy. Cement content (ca. 9–12%) is mainly siderite (Fig. 8h). Framework mineral is dominated by quartz, which makes up ca. 65% of the bulk mineralogy (> 80% of the framework grains). Feldspar in the sample WB-15B

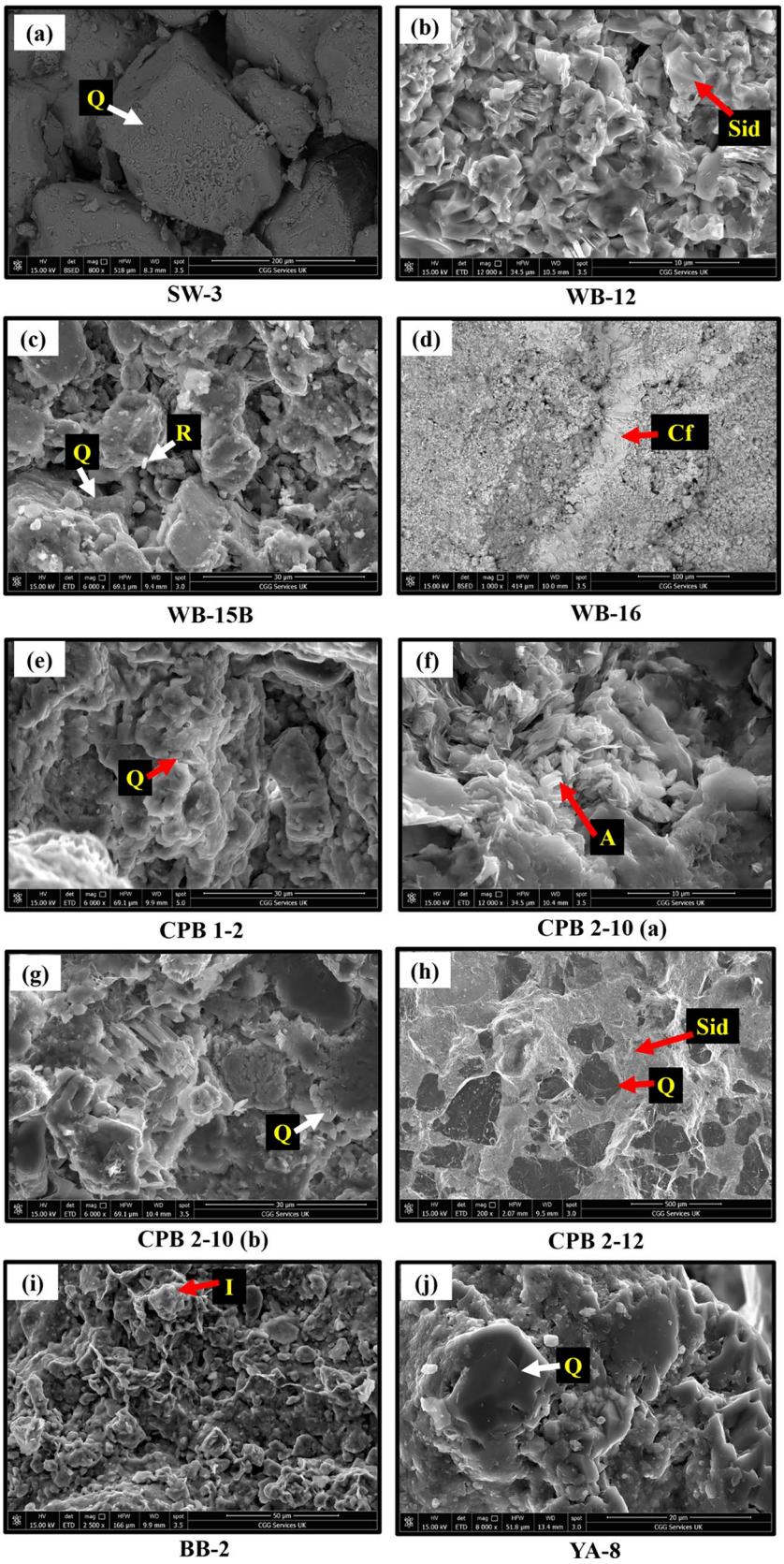

Fig. 8 SEM images of selected samples from the Wessex Basin. Quartz (Q), rutile (R), apatite (A), ilmenite (I), ferroan calcite (Cf) and siderite (Sid). Samples' locations: Swanage (SW), Worbarrow (WB), Compton Bay, older section (CPB-1) and Compton Bay, younger section (CPB-2), Brighstone (BB) and Yaverland (YA)

constitutes < 1% of the bulk mineralogy and is made up of mostly Na-rich plagioclase, as well some amount of intermediate member, andesine. Accessory minerals include rutile (0.06%), zircon (0.03%), ilmenite (0.13%), tourmaline (0.24%), apatite (0.003%), olivine (0.001%), pyroxene (0.001%), monazite (0.001%), and chromite (0.001%) (Appendix 1). Sample CPB-1–2 is a feldspathic wacke (Fig. 10). It has a clay mineral + mica content of ca. 15% while over 90% of the cement is siderite (Tables 1 and 2). Quartz dominates the framework components, constituting over 80% of the framework grains. Feldspar assemblage includes K-feldspars (ca. 2.5% of bulk mineralogy) and plagioclase members, albite (ca. 1.47%), oligoclase (ca. 0.07%, andesine (ca. 0.01%) and bytownite (ca. 0.01%). Heavy minerals include rutile (0.07%), zircon (0.02%), ilmenite (0.05%), tourmaline (0.03%), apatite (0.02%), olivine (0.01%), garnet (0.001%), pyroxene (0.002%), monazite (0.002%), and magnetite (0.001%) (Appendix 1).

The second petrofacies refers to the quartz-rich sandstones (SW-3, WB-12, CPB-2–12, and YA-8) (Figs, 7, 8, 9, 10) and may be further divided into two sub-petrofacies. The first sub-petrofacies (SW-3) is a subarkosic arenite (Fig. 10) containing ca. 90% quartz and > 5% feldspar. Cement formation is minimal (< 2%), with clay mineral + mica content of < 3% (Tables 1 and 2). Feldspar assemblage is dominated by K-feldspar (> 90% of feldspar content). Heavy mineral assemblage comprises of olivine (0.1%), rutile (0.02%), apatite (0.02%), ilmenite (0.01%), tourmaline (0.01%), zircon (0.005%), pyroxene (0.005%), garnet (0.003%), epidote (0–0.002%), and monazite (0.0008%) (Appendix 1). The sub- petrofacies 2 are the quartz arenites (YA-8, WB-12 and CPB-2–12, Figs. 8 and 9). The sample YA-8 contains > 95% quartz. Cement formation is minimal (< 1%), with clay mineral + mica content of ca. 1–3% (Table 1 and 2). Feldspar content is dominated by K-feldspar (> 90% of feldspar content). Heavy mineral assemblage comprises of olivine (0.12%), rutile (0.03%), apatite (0.12%), ilmenite (0.04%), tourmaline (0.02%), and zircon (0.004%) (Appendix 1). Samples WB-12 and CPB-2–12 are iron-rich quartz arenites (Fig. 10). Though their mineral compositions are dominated by quartz (> 95% of the framework elements and ca. 68 and 61% of the bulk mineralogy, respectively), they contain siderite as cement, which makes up over 15% of their bulk mineralogy: ca. 23% and 37%, respectively (Tables 1 and 2). Combined clay mineral and mica content is < 10% of their bulk mineralogy (ca. 8 and 0.8%, respectively). Feldspar is < 1% and is comprised largely of K-feldspars (Tables 1 and 2). Heavy mineral assemblage includes ilmenite (0.07–0.08%), olivine (0.01%), and zircon (0.01%), tourmaline (0.01–0.10%), apatite (0.003–0.01%), rutile (0.002–0.01%), magnetite (0.001–0.002%), and titanite (0–0.001%) (Appendix 1).

5.2 Textural and compositional maturity

Using the textural maturity classification of Nichols (2009), sandstone samples with > 15% matrix/clay + mica content classify as immature, while those with < 5% matrix/clay + mica content are submature to supermature. This classification identifies the wackes (WB-15B and CPB-1–2, Figs. 5 and 6) as texturally immature, the arenites (SW-3 and WB-12, Fig. 5) and (CPB-2–12 and YA-8, Figs. 6 and 7) as texturally submature. The samples from the Wessex Formation (SW-3 and WB-12) are less sorted compared to those from the Vectis Formation (CPB-2–12 and YA-8, Figs. 5 and 7). Maturity indices such as the total quartz to feldspar ratio, monocrystalline to polycrystalline ratio and/or total quartz to feldspar + lithic fragment ratio can be used to describe the compositional maturity of sandstones (Pettijohn, 1975). This means that the Wessex Basin sandstones yield maturity indices that are > 80%, meaning that they are compositionally sub-mature to super-mature.

5.3 Diagenetic modification

The prevalence of floating framework grains and point contacts within the sandstones (Figs. 5 and 7) indicates that there is a limited diagenetic modification to these sandstones. This is also supported by compaction, which is dominated by long, floating and tangential contacts within the grains. It has been documented that Wealden rocks have experienced shallow burial depth of 2 km or less below sea level (Allen, 1975, 1981) with a geothermal gradient that is insufficient to generate adequate heat to cause significant diagenetic alteration (Rollin, 1995; Westaway et al., 2002). In the current study, the formation of carbonate cement in the basin (Fig. 5) also confirms shallow burial depth that aids early-stage diagenesis. Similarly, early diagenetic siderite also occurs as pervasive cement, as well as ooids within the Wessex Basin (Figs. 6e–f, 8). All these lines of evidence confirm that the studied rocks from Wessex Basin have not experienced any significant post-depositional and/or diagenetic alteration and diagenesis is at most limited to the early diagenetic (eodiagenetic) stage.

5.4 Sediments' provenance

The provenance of the sediments in the Wessex Basin sediments is well documented (Allen, 1991). Two prominent sources are generally accepted (Fig. 11): the Cornubian massif in the west as the primary source while Armorica in the southwest is secondary (Allen, 1991, 1998). Other possible sources are the Welsh highlands and London massif (Fig. 11) but evidence for these is not strong (Allen, 1975, 1998). Cornubian massif contained Palaeozoic plutonic granitic rocks, low-grade, regionally metamorphosed

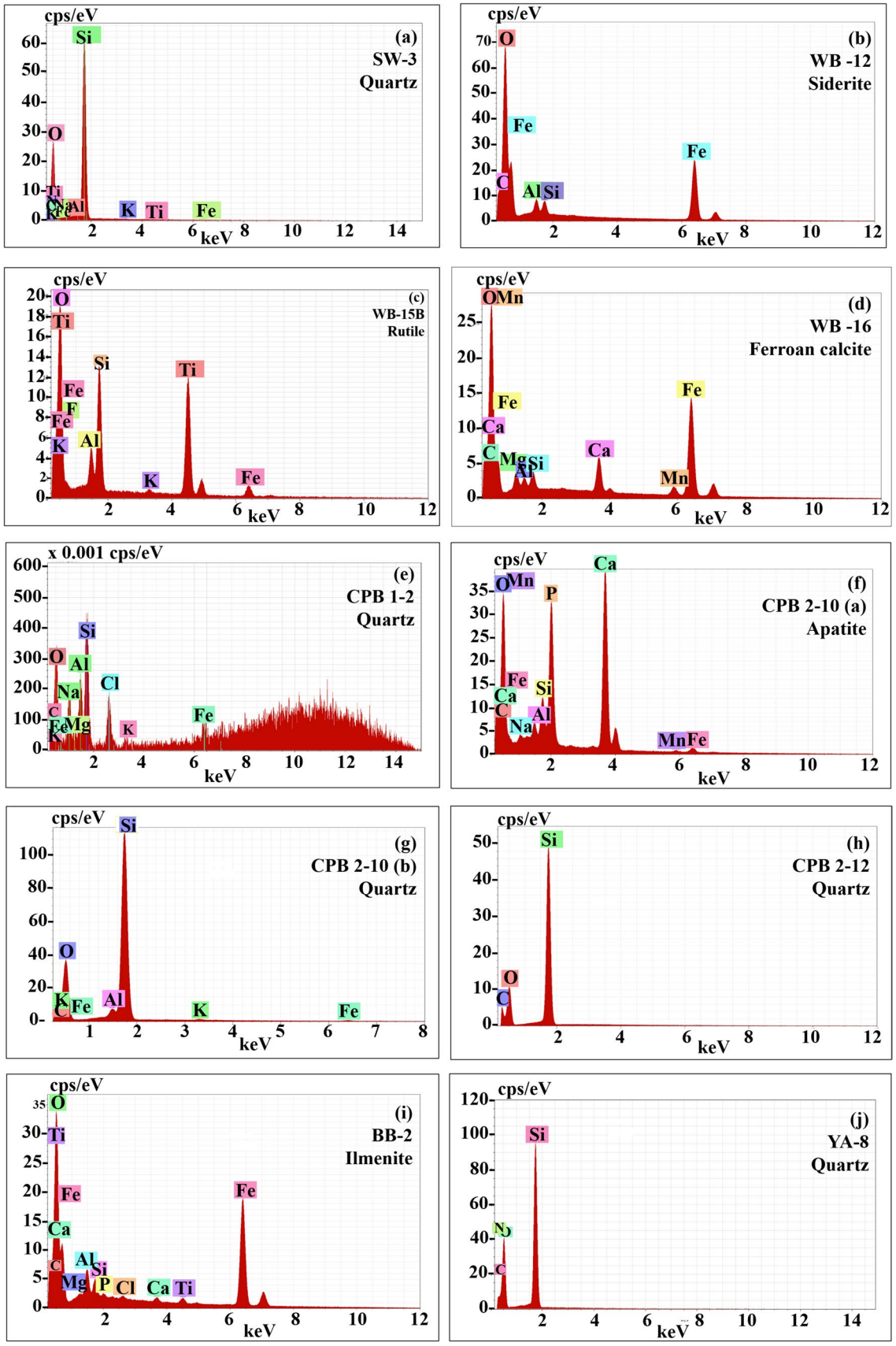
cps/eV
(a)
SW-3
Quartz
Si
O
Ti
Al
K
Ti
Fe
keV
cps/eV
(b)
WB -12
Siderite
O
Fe
C
Al
Si
Fe
keV
cps/eV
(c)
WB-15B
Rutile
O
Ti
Si
Ti
Fe
F
Fe
K
Al
K
Fe
keV
cps/eV
(d)
WB -16
Ferroan calcite
OMn
Fe
Ca
Fe
C
Mg
Si
Ca
Mn
keV
x 0.001 cps/eV
(e)
CPB 1-2
Quartz
Si
O
Al
Na
Cl
C
Fe
Mg
K
K
Fe
keV
cps/eV
(f)
CPB 2-10 (a)
Apatite
Ca
OMn
P
Fe
Ca
Si
C
Al
Na
Mn
Fe
keV
cps/eV
(g)
CPB 2-10 (b)
Quartz
Si
O
K
C
Fe
Al
K
Fe
keV
cps/eV
(h)
CPB 2-12
Quartz
Si
O
C
keV
cps/eV
(i)
BB-2
Ilmenite
O
Ti
Fe
Fe
Ca
C
Al
Si
Mg
P
Cl
Ca
Ti
keV
cps/eV
(j)
YA-8
Quartz
Si
Na
C
keV

◂**Fig. 9** EDS spectra of selected minerals in the samples from the Wessex Basin. Quartz (Q), rutile (R), apatite (A), ilmenite (I), ferroan calcite (Cf), and siderite (Sid). Samples' locations: Swanage (SW), Worbarrow (WB), Compton Bay, older section (CPB-1) and Compton Bay, younger section (CPB-2), Brighstone (BB) and Yaverland (YA)

Devonian-Carboniferous volcanics and sediments (Allen, 1972b, 1991; Darbyshire & Shepherd, 1994). The major rock groups within the Cornubian massif are granites, shales, sandstones, cherts limestones, volcanics, (Hall, 1990). The granites have significant amount of quartz, plagioclase, and K-feldspar, biotite and muscovite and the massif was a major source of tourmaline-rich materials (Allen, 1972b, 1991). On the other hand, the Armorican massif consist Precambrian core of staurolite-kyanite-garnet schists, granites, Permo-Triassic New Red Sandstone and minor Mesozoic rocks that supplied Jurassic volcanogenic fragments (Allen, 1991, 1998). The massif supplied high-grade metamorphic materials and are rich in garnet and apatite (Allen, 1991, 1998). Heavy mineral suites confirm the overwhelming predominance of Cornubian materials over Armorican and other sources within the section at Swanage (Allen, 1972a, 1972b) while the presence of coarse quartz grit at Worbarrow Bay indicates sourcing as a result of uplift of Cornubia (Allen, 1989). At Compton Bay and Brighstone, detrital petrography of the sand fraction indicates sourcing from eastern Cornubia that exposed mainly Permian–Triassic red beds with fringing Jurassic sediments as granite was not exposed (Allen, 1998). On the other hand, Late Precambrian pebble at Yaverland indicates primary derivation from the Armorican massif and secondary recycling via Permian–Triassic pebble beds, probably on the eastern flanks of the Cornubian massif (Allen, 1975). In the current study, the dominance of monocrystalline quartz grains within the sandstones (Figs. 7, 8, 9) and the observed lithic fragments indicate a plutonic or high-grade metamorphic source (Basu, 1985). However, the significant concentrations of heavy mineral suite of garnet and rutile (Figs. 6 and 7) indicate metamorphic origin for the sediments within the Wessex Basin (Fossum et al., 2019). This raises the possibility of mixture of metamorphic and igneous materials at the source areas although the current datasets are not sufficient to decide whether metamorphic sources are primary or secondary. However, Akinlotan and Rogers (2021) have used detailed analyses of heavy mineral assemblages: high Garnet: Zircon index (GZi) values (garnet*100/garnet + zircon), the presence of epidote and a garnet assemblage that is dominated by almandine and grossular to imply that the sediments from the Wessex Basin were mainly derived from metamorphic sources with the possibility of minor contributions from igneous sources.

The dominance of quartz within the grain framework coupled with the small concentration of feldspar and fragments (Figs. 7, 8, 9, 10) indicates that these sediments were recycled from older sedimentary materials in the source areas discussed above (Dickinson, 1985). This conclusion is supported by the maturity and the transportation of the sandstones (Figs. 5 and 7). The shape and angularity of grains can indicate sediment transport history (Akinlotan et al., 2021a; Dickinson, 1985; Jenchen, 2018) and the shape and sorting of the grains (Figs. 5 and 7) reveal that the sandstones are generally matured texturally and compositionally (Dickinson, 1985; Jenchen, 2018; Mohammedyasin & Wudie, 2019). Similarly, the prevalence of angular to sub-rounded grains in the sandstones (Figs. 7–10) indicates a short transport distance from the source area to the site of deposition (Jenchen, 2018; Mohammedyasin & Wudie, 2019). The major source massif for the Wessex Basin is Cornubia (Fig. 11) and is about 110 km west from the basin (Allen & Wimbledon, 1991; Sweetman & Goodyear, 2020) while Armorican massif (Fig. 11) the secondary source is closer to the basin than Cornubia (Radley & Allen, 2012a). It is important to note that significant amount of travel (more than 110 km) would be required to produce quartz-rich sandstones by removing feldspar and unstable minerals through significant sediment transportation (Basu, 1985; Dickinson, 1985; Franzinelli & Potter, 1983). In terms of sediment transport and change in sandstone composition over the course of transport history, comparison can be drawn between the Wessex Basin on one hand and sands in the Platte River in Nebraska, USA and Amazon River based on similarity in sediment transport and composition. In the Platte River sands in Nebraska, USA (Bryer & Bart, 1978), a travel distance of 600 km was insufficient to significantly change the ratio of quartz: feldspar. Similarly, it required a travel distance of about 4000 km to significantly increase the quantity of quartz to feldspar in the Amazon River sands (Franzinelli & Potter, 1983). This means that a travel distance of about 110 km from the Cornubian massif and lesser distance from the Armorica would not be enough to produce the quartz-rich sands observed in the Wessex Basin. Hence, the sands are likely to have been recycled from older sedimentary materials within the source areas. The substantial concentrations of rutile, tourmaline, zircon and ilmenite within the heavy mineral assemblages (Figs. 6, 8 and 9, Appendix 1) also confirm that the sediments were recycled from older sediments within the provenance. The concentration of ZTR index: Zircon: Tourmaline: Rutile index ((ziron + tourmaline + rutile)*100/total transparent heavy minerals) has been used to indicate sediment reworking (Aubrecht et al., 2017; Fossum et al., 2019; Mange & Morton, 2007). Akinlotan and Rogers (2021) reported high ZTR index values (from 25 to 50%) for the Wessex Basin rocks and this also suggests a high amount of sediment reworking from sedimentary materials in the source areas before being deposited in the basin. Reworking of materials

Table 2 Summary of the bulk mineralogy of the samples from the Wessex Basin based on QEMSCAN®

Mineral components		Locations								
		SW-3 (%)	WB-12 (%)	WB-15B (%)	WB-16 (%)	CPB-1-2 (%)	CPB-2-10 (%)	CPB-2-12 (%)	BB-2 (%)	YA-8 (%)
Quartz	Mono	82.20	61.69	61.73	13.24	64.22	46.13	61.36	52.77	95.80
	Poly	9.10	6.85	3.35	-	3.38		-	-	2.00
K-Feldspar		5.06	0.01	0.00	0.35	2.54	0.36	0.23	1.22	0.20
Plagioclase		0.20	0.01	0.00	0.35	1.55	3.13	0.00	0.74	0.00
Clay minerals		1.99	7.60	18.32	7.77	13.61	24.84	0.68	39.37	1.16
Micas		0.51	0.72	3.55	0.81	1.45	4.60	0.14	4.17	0.05
Cements		0.77	22.91	9.32	76.67	0.22	15.89	37.48	1.36	0.56
Heavy minerals		0.17	0.21	0.45	0.89	0.20	5.05	0.11	0.37	0.23

Sandstone | Ironstone | Mudstone

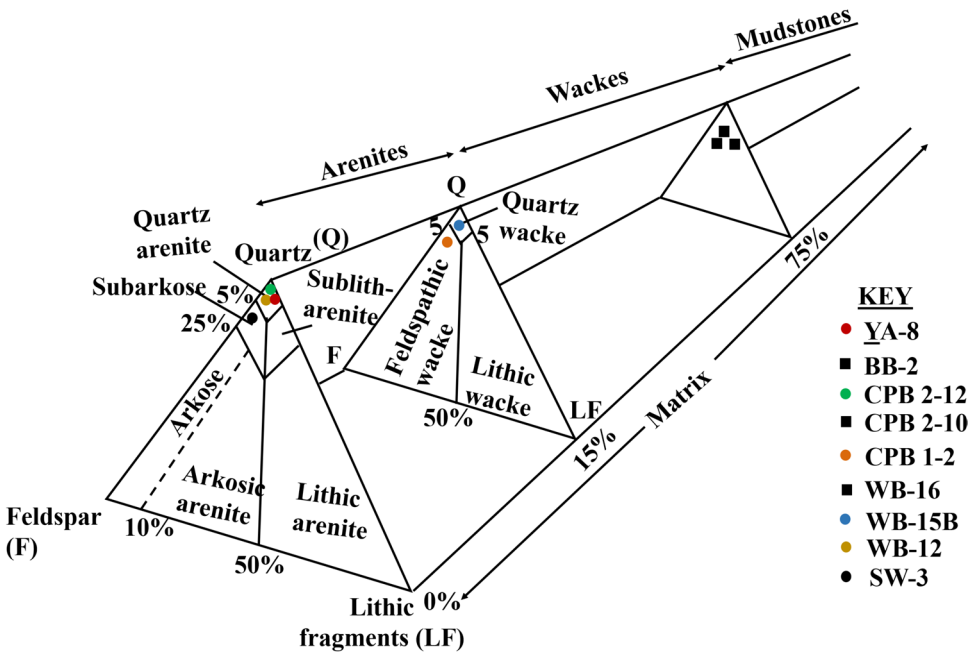

Fig. 10 Ternary diagram showing the composition of the sandstone from the Wessex Basin (after (Pettijohn et al., 1987). Circle plots indicate sandstones, while square plots indicate mudstones. Samples' locations: Swanage (SW), Worbarrow (WB), Compton Bay, older section (CPB-1) and Compton Bay, younger section (CPB-2), Brighstone (BB) and Yaverland (YA)

in the source areas may either indicate primary or secondary recycling (Caracciolo, 2020; Garzanti, 2016). Primary recycling would mean sourcing from the older basement igneous and/or metamorphic rocks while secondary recycling would indicate sourcing from older sedimentary rocks within the massifs (Caracciolo, 2020; Garzanti, 2016). However, all pieces of evidence described from the current study suggest that most of the Wessex Basin sediments were reworked from older sedimentary materials in the source areas indicating secondary recycling within the massifs.

The composition of sandstones can be used to determine the nature of tectonic settings of their provenance (Dickinson, 1985; Dickinson & Suczek, 1979). Quartz-rich sands with a very high ratio of monocrystalline to polycrystalline grains and a high ratio of K-feldspar to plagioclase feldspar may be indicative of sourcing from a stable craton/passive platform (Dickinson, 1985; Dickinson & Suczek, 1979). In the current study, the dominance of quartz over other framework grains, as well as a minor concentration of feldspar that is comprised of mostly K-feldspars (Figs. 7, 8, 9, 10)

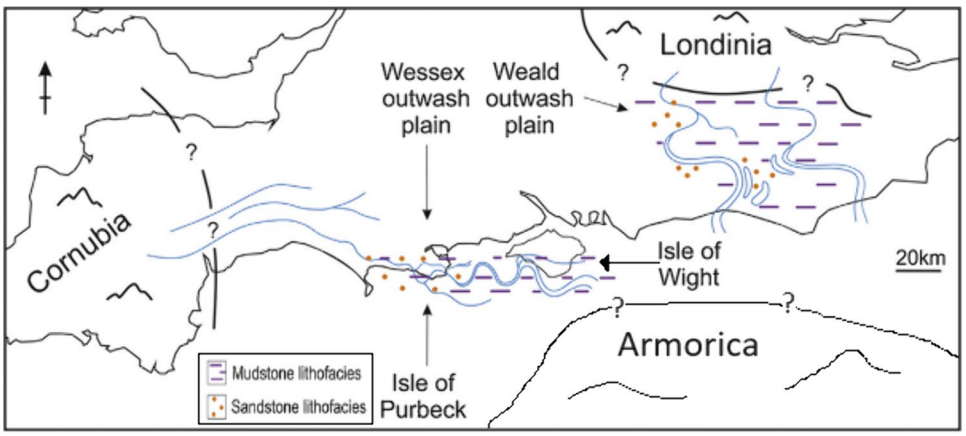

Fig. 11 Palaeogeography of the Early Cretaceous times showing source massifs, Wealden facies and basins after Penn et al. (2020)

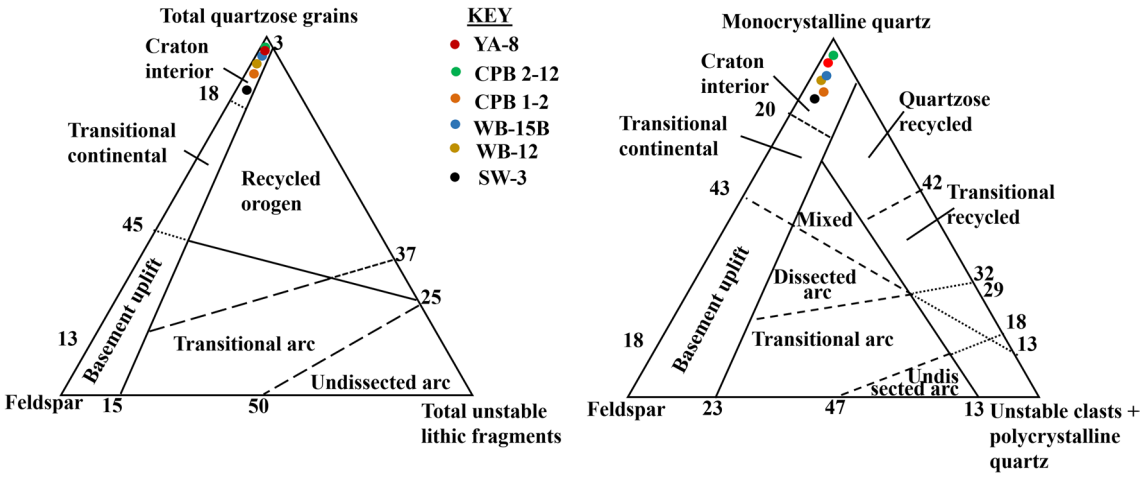

Fig. 12 Ternary diagrams showing the provenance of the sandstones of the Wessex Basin after Dickinson et al. (1983). Samples' locations: Swanage (SW), Worbarrow (WB), Compton Bay, older section (CPB-1) and Compton Bay, younger section (CPB-2), Brighstone (BB) and Yaverland (YA)

suggests that the materials within the Wessex Basin were sourced from stable continental craton. This conclusion is supported by the fact that the sandstone samples from the current study plot within the Craton interior (Fig. 12) of Dickinson et al. (1983). It has been shown that stable continental craton is largely composed of felsic plutonic igneous and metamorphic rock that produce quartzose sands, with minor feldspars (Boggs Jr, 2009; Dickinson, 1985) that have been observed in the studied sandstones.

5.5 Palaeoclimate and weathering

The low concentration of unstable materials such as K-feldspar, plagioclase, biotite, and muscovite (Figs. 5 and 7, Table 2) in the Wessex Basin may indicate hot and moist palaeoclimatic conditions that favoured intense weathering patterns at source areas (Akinlotan et al., 2021a; Dickinson, 1985). Similarly, the submature to supermature nature of the sandstones (Figs. 5 and 7) reflects climatic conditions that favoured weathering and transport processes that have removed most of the unstable grains (Akinlotan et al., 2021a; Dickinson, 1985). The presence of ultra-stable heavy minerals such as rutile, tourmaline, zircon and ilmenite within the sandstones (Figs. 6, 8 and 9) also indicates a high degree of weathering conditions within moist and warm climatic conditions at the source areas (Aubrecht et al., 2017; Fossum et al., 2019).

Clay mineral studies of the Wessex rocks reveals illite (a product of mechanical weathering of aluminosilicate minerals) as the dominant clay mineral (Appendix 1). Further studies of these products of weathered feldspars in the basin, revealed that the palaeoclimate was likely a predominantly arid one with short, intermittent warm but wet seasons (Akinlotan et al., In press). Previous studies have also shown that the climate of the source area tended towards aridity (Ruffell & Batten, 1990; Ruffell

& Rawson, 1994), hence the weathering of feldspars was more of a mechanical process than chemical. However, the occurrence of intermittent warm and wet seasons, also allowed for chemical weathering to take place (Akinlotan et al., In press). Hence, the preservation of some feldspars within the Wessex Basin (Figs. 5 and 7) suggests that chemical weathering was likely moderate, as opposed to being intense. However, since most of the sediments within the Wessex Basin have been recycled and travelled comparably less distance, weathering patterns may be physical, chemical or a combination of both. The presence of zircon (Fig. 6), a weathering-resistant mineral within the sandstones may indicate severe weathering that resulted from seasonal humid conditions at source areas (Dickinson, 1985; Hurford et al., 1984). The chemical weathering of feldspars into clays probably occurred at the source before the rocks were deposited while the physical breakdown of the rocks probably happened during transportation as observed in their textural maturity (Sladen & Batten, 1984).

5.6 Depositional environments

Previous studies of the rocks within the Wessex Basin using different proxies have shown that depositional environments range from fluvial to lagoonal settings for the Wessex and Vectis formations, respectively (e.g. Radley & Barker, 1998a, 2000; Stewart et al., 1991; Stewart, 1981a, 1981b). The mineralogy of the rock samples (Figs. 6–7) from the current study reveals some pieces of evidence that agree with this interpretation. The quartz-rich sandstones (SW-3 and YA-8), both have > 95% quartz, which qualify them as arenites (Fig. 10). The iron-rich sandstones also have similar mineralogical composition (Fig. 10). A close look at individual mineralogy reveals that samples SW-3 and WB-12 from the Wessex Formation (Fig. 5) have more angular grains, polycrystalline quartz, clay minerals, and feldspars than the samples CPB-2–12 and YA-8 from the Vectis Formation (Fig. 6). Angularity of grains suggests a lesser amount of attrition on the grains and for grains to become rounded, a higher amount of attrition process, either by water or wind waves is required (Selley, 1996). Hence, the angular nature of the SW-3 grains (Figs. 6, 7, 8) most likely indicates deposition in a fluvial environment (Selley, 1996). Similarly, it is suggested that the wave currents that influenced the sandstone (YA-8), had a greater winnowing effect that weathered the unstable mineral grains such as feldspars and polycrystalline quartz, and depleted clay content. However, for the sandstone (SW-3), the fluvial current most likely had a lesser winnowing effect, hence the higher amount of unstable minerals and clay. This lesser winnowing effect may also explain why the quartz wacke samples (WB-15B and CPB-1–2), with up to 15% clay + mica content are limited to the Wessex Formation.

Textural maturity ranges from submature in the older samples (e. g. SW-3 and WB-12), to immature in the samples from the younger parts of the Wessex Formation, WB-12 and CPB-1–2 (Figs. 6, 7). Textural maturity in sandstones reflect the depositional energy of the transporting medium. This means that the energy level of the transporting medium experienced a decline by the time the younger sandstones (WB-12 and CPB-1–2) were deposited, causing a higher clay content in the sandstones. This is comparable to a river setting where the depositional energy continues to wane as the river moves out from the source (Selley, 1996). As the energy drops, attrition and winnowing effect reduces, allowing for the occurrence of angular and unstable grains, as well as clay in considerable quantities (Selley, 1996). On the other hand, the samples from the Vectis Formation are texturally mature (Figs. 7 and 9). The high detrital quartz content, with more rounded shapes, in addition to the minor clay and feldspar content, reflects the high amount of attrition and winnowing-out of unstable minerals during transport and deposition (Pettijohn, 1975; Pettijohn et al., 1987).

6 Significance of study

Although the Wessex Basin has been the focus of extensive sedimentological and palaeontology studies (e.g. Radley & Barker, 1998a, 2000; Radley et al., 1998a, 1998b; Stewart, 1978, 1981b; Sweetman & Insole, 2010; Sweetman & Underwood, 2006), mineralogical and petrographic studies within the Wessex Basin are very limited in the literature. This current study has presented comprehensive petrographic and mineralogical datasets for the Wessex Basin to validate previous interpretations made from sedimentology and palaeontology datasets. This is the only study as far as we know that have used an integrated approach (optical microscopy, scanning electron microscopy, energy dispersive spectrometry and Quantitative Evaluation of Minerals by Scanning Electron Microscopy) in a single study to conduct mineralogical and petrographic descriptions of the sediments within the Wessex Basin. The interpretations made from the mineralogical and petrographic datasets from this study agree with the findings of previous interpretations using different proxies (e.g., Stewart, 1981a, 1981b; Lake and Shephard-Thorn, 1987; Ross, 1996). This confirms the reliability and suitability of mineralogy and petrography for interpreting paleoenvironmental and depositional conditions. As a result, the methodology and the datasets used in this study could be used in other non-marine Lower Cretaceous

facies e. g. Western Interior Basin, North American (Sames et al., 2010), Kyongsang Basin, Korea (Jo, 2003), Tataouine Basin, Southern Tunisia (Anderson et al., 2007), Escucha Formation, eastern Spain (Tibert et al., 2013), Xiazhuang Formation, north China (Pan & Zhu, 2007), and the Jinju Formation, South Korea (Choi & Huh, 2016), and elsewhere (e.g. Haywood et al., 2004).

7 Conclusion

This study uses an integrated approach to study mineralogical and petrographic compositions of selected samples from the Wessex Basin, southeast England with the aim of making palaeoenvironmental interpretations. The sandstones were identified as feldspathic and quartz wackes, subarkose and quartz arenites. The results revealed a high quartz content with little feldspar content that is largely K-feldspars and Na-rich plagioclase. Heavy minerals contents include rutile, tourmaline, zircon, apatite, ilmenite, olivine, amphibole, pyroxene, magnetite, monazite, epidote, and garnet. With a loose packing and pervasive siderite cement, the sandstones experienced no significant diagenetic alteration. Texturally and compositionally, the sandstone maturity ranged from immature to supermature, reflecting the environmental processes that influenced the sediments during deposition. The compositional submature to supermature nature of the sandstones is linked to their provenance and the palaeoclimatic conditions that facilitated the weathering process. The high monocrystalline quartz content, with subordinate K-feldspars and heavy mineral concentration suggests mixture of metamorphic and igneous materials at the source areas.

Supplementary Information The online version contains supplementary material available at https://doi.org/10.1007/s43217-024-00194-6.

Acknowledgements OOA wishes to express gratitude to CGG Robertson, North Wales for providing collaborative funding for the laboratory analyses for this study. Gareth Rogers and Elisha Drumm of CGG Robertson, North Wales are thanked for conducting laboratory analyses (QEMSCAN®, SEM and optical microscopy). Many thanks to Mr Alan Holiday for helping us to identify suitable locations for field studies at Dorset. We appreciate the reviewers and editor for providing constructive comments and suggestions that improved the quality of the final manuscript.

Author contribution OOA: Conceptualization and Design, Field studies and Sampling, Investigation, Validation, Writing – original draft preparation, Writing- Reviewing and Editing, Supervision and administration. OAMoghalu: Writing – original draft preparation, Writing-Reviewing and Editing OAA: Writing- Reviewing and Editing. All authors reviewed the manuscript.

Data availability Supplementary material is available as appendix 1 and the corresponding author can be contacted for queries or clarifications regarding this.

Declarations

Conflict of interest We declare that we have no conflict of interest regarding our submission. We do not have any financial or non-financial interests that are directly or indirectly related to the work.

References

Akinlotan, O. O., Moghalu, O. A., Hatter, S. J., Jolly, B. A., Anyiam, O. A. In press. Palaeoclimatic and palaeoenvironmental controls on clay mineral distribution in the Early Cretaceous (Barremian): the Wessex Basin, southeast England. *Journal of Earth Science*. (**Accepted**)

Adams, A., Guilford, C., & MacKenzie, W. (1984). *Atlas of sedimentary rocks under the microscope*. Essex, United Kingdom: Longman Group UK Ltd.

Akinlotan, O. O. (2015). *The Sedimentology of the Ashdown Formation and the Wadhurst Clay Formation* (p. 258). University of Brighton, United Kingdom.

Akinlotan, O. O. (2016). Porosity and permeability of the English (Lower Cretaceous) sandstones. *Proceedings of the Geologists' Association, 127*, 681–690.

Akinlotan, O. O. (2017a). Geochemical analysis for palaeoenvironmental interpretations – a case study of the English Wealden (Lower Cretaceous, southeast England). *Geological Quarterly, 61*, 227–238.

Akinlotan, O. O. (2017b). Mineralogy and palaeoenvironments: The Weald Basin (Early Cretaceous), Southeast England. *The Depositional Record, 3*, 187–200.

Akinlotan, O. O. (2018). Multi-proxy approach to palaeoenvironmental modelling: The English Lower Cretaceous Weald Basin. *Geological Journal, 53*, 316–335.

Akinlotan, O. O. (2019). Sideritic ironstones as indicators of depositional environments in the Weald Basin (Early Cretaceous) SE England. *Geological Magazine, 156*, 533–546.

Akinlotan, O. O., Adepehin, E. J., Rogers, G. H., & Drumm, E. C. (2021a). Provenance, palaeoclimate and palaeoenvironments of a non-marine Lower Cretaceous facies: Petrographic evidence from the Wealden Succession. *Sedimentary Geology, 415*, 105848.

Akinlotan, O. O., & Hatter, S. J. (2022). Depositional controls on diagenetic evolution of the Lower Cretaceous Wealden Sandstones (Wessex Basin, southeast England). *Marine and Petroleum Geology, 146*, 105948.

Akinlotan, O. O., Moghalu, O. A., Hatter, S. J., Okunuwadje, S. E., Anquilano, L., Onwukwe, U., Haghani, S., Anyiam, O. A., & Jolly, B. A. (2022). Clay mineral formation and transformation in non-marine environments and implications for Early Cretaceous palaeoclimatic evolution: the Weald Basin, southeast England. *Journal of Palaeogeography, 11*(3), 387–409.

Akinlotan, O. O., & Rogers, G. H. (2021). Heavy mineral constraints on the provenance evolution of the English Lower Cretaceous (Wessex Basin). *Marine and Petroleum Geology, 1287*, 104952.

Akinlotan, O. O., Rogers, G. H., & Okunuwadje, S. E. (2021b). Provenance evolution of the english Lower Cretaceous weald basin and implications for palaeogeography of the northwest European massifs: constraints from heavy mineral assemblages. *Marine and Petroleum Geology, 127*, 104953.

Allen, P. (1972a) Transitional sandstones-the Wealden of southern England, National conference on earth science- arenaceous deposits- sedimentation, (pp. 179–202).

Allen, P. (1948). Wealden petrology : the top ashdown pebble bed and the top ashdown sandstone. *Quarterly Journal of the Geological Society, 104*, 257–321.

Allen, P. (1959). The wealden environment: Anglo-Paris Basin. Philosophical transactions of the royal society of London. *Series b, Biological Sciences, 242*(692), 283–346.

Allen, P. (1967). Origin of the hastings facies in North-western Europe. *Proceedings of the Geologists' Association, 78*, 27-IN66.

Allen, P. (1972b). Wealden detrital tourmaline: Implications for northwestern Europe. *Journal of the Geological Society, 128*, 273–294.

Allen, P. (1975). Wealden of the Weald: A new model. *Proceedings of the Geologists' Association, 86*, 389–437.

Allen, P. (1981). Pursuit of Wealden models. *Journal of the Geological Society, 138*, 375–405.

Allen, P. (1989). Wealden research—ways ahead. *Proceedings of the Geologists' Association, 100*, 529–564.

Allen, P. (1991). Provenance research: Torridonian and Wealden. *Geological Society, London, Special Publications, 57*, 13–21.

Allen, P. (1998). Purbeck-Wealden (early Cretaceous) climates. *Proceedings of the Geologists' Association, 109*, 197–236.

Allen, P., Keith, M., Tan, F., & Deines, P. (1973). Isotopic ratios and Wealden environments. *Palaeontology, 16*, 607.

Allen, P., & Krumbein, W. (1962). Secondary trend components in the top Ashdown pebble bed: A case history. *The Journal of Geology, 70*, 507–538.

Allen, P., & Wimbledon, W. (1991). Correlation of NW European Purbeck-Wealden (nonmarine Lower Cretaceous) as seen from the English type-areas. *Cretaceous Research, 12*, 511–526.

Anderson, P. E., Benton, M. J., Trueman, C. N., Paterson, B. A., & Cuny, G. (2007). Palaeoenvironments of vertebrates on the southern shore of Tethys: The nonmarine Early Cretaceous of Tunisia. *Palaeogeography, Palaeoclimatology, Palaeoecology, 243*, 118–131.

Aubrecht, R., Sýkora, M., Uher, P., Li, X.-H., Yang, Y.-H., Putiš, M., & Plašienka, D. (2017). Provenance of the Lunz Formation (Carnian) in the Western Carpathians, Slovakia: Heavy mineral study and in situ LA–ICP–MS U-Pb detrital zircon dating. *Palaeogeography, Palaeoclimatology, Palaeoecology, 471*, 233–253.

Basu, A. (1985). Influence of climate and relief on compositions of sands released at source areas. In G. G. Zuffa (Ed.), *Provenance of arenites* (pp. 1–18). Springer.

Boggs, S., Jr. (2009). *Petrology of sedimentary rocks*. Cambridge University Press.

Bryer, J. A., & Bart, H. A. (1978). The composition of fluvial sands in a template semi-arid region. *Journal of Sedimentary Research, 48*, 1311–1320.

Caracciolo, L. (2020). Sediment generation and sediment routing systems from a quantitative provenance analysis perspective: Review, application and future development. *Earth-Science Reviews, 209*, 103226.

Choi, B.-D., & Huh, M. (2016). Mongolocypris kohi sp. nov.: A new Early Cretaceous non-marine ostracod species from the Jinju Formation. *South Korea. Cretaceous Research, 57*, 239–247.

Daley, B., & Stewart, D. J. (1979). Week-end field meeting: The Wealden Group in the Isle of Wight 17–19 June 1977. *Proceedings of the Geologists' Association, 90*, 51–54.

Darbyshire, D., & Shepherd, T. (1994). Nd and Sr isotope constraints on the origin of the Cornubian batholith, SW England. *Journal of the Geological Society, 151*, 795–802.

De Segonzac, G. D. (1970). The transformation of clay minerals during diagenesis and low-grade metamorphism: A review. *Sedimentology, 15*, 281–346.

Dickinson, W. R. (1985). Interpreting provenance relations from detrital modes of sandstones. In G. G. Zuffa (Ed.), *Provenance of arenites* (pp. 333–361). Springer.

Dickinson, W. R., Beard, L. S., Brakenridge, G. R., Erjavec, J. L., Ferguson, R. C., Inman, K. F., Knepp, R. A., Lindberg, F. A., & Ryberg, P. T. (1983). Provenance of North American Phanerozoic sandstones in relation to tectonic setting. *Geological Society of America Bulletin, 94*, 222–235.

Dickinson, W. R., & Suczek, C. A. (1979). Plate tectonics and sandstone compositions. *AAPG Bulletin, 63*, 2164–2182.

Eberl, D. D. (1984). Clay mineral formation and transformation in rocks and soils [and discussion]. philosophical transactions of the Royal Society of London. *Series a, Mathematical and Physical Sciences, 311*, 241–257.

Fang, Q., Hong, H., Zhao, L., Furnes, H., Lu, H., Han, W., Liu, Y., Jia, Z., Wang, C., & Yin, K. (2017). Tectonic uplift-influenced monsoonal changes promoted hominin occupation of the Luonan Basin: Insights from a loess-paleosol sequence, eastern Qinling Mountains, central China. *Quaternary Science Reviews, 169*, 312–329.

Folk, R. L. (1980). *Petrology of Sedimentary Rocks*. Austin: Hemphiliîs.

Fossum, K., Morton, A. C., Dypvik, H., & Hudson, W. E. (2019). Integrated heavy mineral study of Jurassic to Paleogene sandstones in the Mandawa Basin, Tanzania: Sediment provenance and source-to-sink relations. *Journal of African Earth Sciences, 150*, 546–565.

Franzinelli, E., & Potter, P. E. (1983). Petrology, chemistry, and texture of modern river sands, Amazon River system. *The Journal of Geology, 91*, 23–39.

Garzanti, E. (2016). From static to dynamic provenance analysis—Sedimentary petrology upgraded. *Sedimentary Geology, 336*, 3–13.

Hall, A. (1990). Geochemistry of the Cornubian tin province. *Mineralium Deposita, 25*, 1–6.

Haywood, A. M., Valdes, P. J., & Markwick, P. J. (2004). Cretaceous (Wealden) climates: A modelling perspective. *Cretaceous Research, 25*, 303–311.

Hopson, P., Wilkinson, I., Woods, M. (2008) A stratigraphical framework for the Lower Cretaceous of England. British Geological Survey, (p. 77).

Hurford, A., Fitch, F., & Clarke, A. (1984). Resolution of the age structure of the detrital zircon populations of two Lower Cretaceous sandstones from the Weald of England by fission track dating. *Geological Magazine, 121*, 269–277.

Insole, A. N., & Hutt, S. (1994). The palaeoecology of the dinosaurs of the Wessex Formation (Wealden Group, Early Cretaceous), Isle of Wight, Southern England. *Zoological Journal of the Linnean Society, 112*, 197–215.

Jenchen, U. (2018). Petrography and geochemistry of the Triassic El Tranquilo Group, Deseado Massif, Patagonia, Argentina: Implications for provenance and tectonic setting. *Journal of South American Earth Sciences, 88*, 530–550.

Jo, H. (2003). Depositional environments, architecture, and controls of Early Cretaceous non-marine successions in the northwestern part of Kyongsang Basin, Korea. *Sedimentary Geology, 161*, 269–294.

Kemp, S., Wagner, D., Ingham, M. (2012) The mineralogy, surface area and geochemistry of samples from the Wealden Group of southern England. British Geological Survey Internal Report, IR/10/079, (p. 34).

Kim, J., Dong, H., Seabaugh, J., Newell, S. W., & Eberl, D. D. (2004). Role of microbes in the smectite-to-illite reaction. *Science, 303*, 830–832.

Knappett, C., Pirrie, D., Power, M., Nikolakopoulou, I., Hilditch, J., & Rollinson, G. (2011). Mineralogical analysis and provenancing of ancient ceramics using automated SEM-EDS analysis (QEMSCAN®): A pilot study on LB I pottery from Akrotiri, Thera. *Journal of Archaeological Science, 38*, 219–232.

Lake, S. D., & Karner, G. D. (1987). The structure and evolution of the Wessex Basin, southern England: An example of inversion tectonics. *Tectonophysics, 137*, 347–378.

Mange, M. A., & Morton, A. C. (2007). Geochemistry of heavy minerals. *Developments in Sedimentology, 58*, 345–391.

Mohammedyasin, M. S., & Wudie, G. (2019). Provenance of the Cretaceous Debre Libanos sandstone in the Blue Nile Basin, Ethiopia: Evidence from petrography and geochemistry. *Sedimentary Geology, 379*, 46–59.

Nichols, G. (2009). *Sedimentology and Stratigraphy*. Wiley-Blackwell.

Nie, J., & Peng, W. (2014). Automated SEM–EDS heavy mineral analysis reveals no provenance shift between glacial loess and interglacial paleosol on the Chinese Loess Plateau. *Aeolian Research, 13*, 71–75.

Osborne White, H. J. (1921) Geology of the Isle of Wight. Memoir of the Geological Survey of Great Britain (England and Wales), (pp. 1–219).

Pan, H., & Zhu, X. (2007). Early Cretaceous non-marine gastropods from the Xiazhuang Formation in North China. *Cretaceous Research, 28*, 215–224.

Penn, S. J., Sweetman, S. C., Martill, D. M., & Coram, R. A. (2020). The Wessex Formation (Wealden Group, Lower Cretaceous) of Swanage Bay, southern England. *Proceedings of the Geologists' Association, 131*, 679–698.

Pereda-Suberbiola, J. (1993). Hylaeosaurus, polacanthus, and the systematics and stratigraphy of Wealden armoured dinosaurs. *Geological Magazine, 130*, 767–781.

Pettijohn, F. (1975). *Sedimentary rocks*. New York: Harper & Row.

Pettijohn, F., Potter, P. E., & Siever, R. (1987). *Sand and sandstone*. NY: Springer Science & Business Media.

Pirrie, D., Power, M. R., Rollinson, G. K., Wiltshire, P. E., Newberry, J., & Campbell, H. E. (2009). Automated SEM-EDS (QEMSCAN®) Mineral analysis in forensic soil investigations: Testing instrumental reproducibility. *Criminal and Environmental Soil Forensics* (pp. 411–430). Dordrecht: Springer.

Radley, J. D., & Allen, P. (2012a). The non-marine Lower Cretaceous Wealden strata of southern England. *Proceedings of the Geologists' Association, 123*, 235–244.

Radley, J. D., & Allen, P. (2012b). The Wealden (non-marine Lower Cretaceous) of the Wessex Sub-basin, southern England. *Proceedings of the Geologists' Association, 123*, 319–373.

Radley, J. D., & Barker, M. J. (1998a). Palaeoenvironmental analysis of shell beds in the Wealden Group (Lower Cretaceous) of the Isle of Wight, southern England: An initial account. *Cretaceous Research, 19*, 489–504.

Radley, J. D., & Barker, M. J. (1998b). Stratigraphy, palaeontology and correlation of the Vectis Formation (Wealden Group, Lower Cretaceous) at Compton Bay, Isle of Wight, southern England. *Proceedings of the Geologists' Association, 109*, 187–195.

Radley, J. D., & Barker, M. J. (2000). Molluscan palaeoecology and biostratinomy in a Lower Cretaceous meanderplain succession (Wessex Formation, Isle of Wight, southern England). *Proceedings of the Geologists' Association, 111*, 133–145.

Radley, J. D., Barker, M. J., & Harding, I. C. (1998a). Palaeoenvironment and taphonomy of dinosaur tracks in the Vectis Formation (Lower Cretaceous) of the Wessex Sub-basin, southern England. *Cretaceous Research, 19*, 471–487.

Radley, J. D., Gale, A. S., & Barker, M. J. (1998b). Derived Jurassic fossils from the vectis formation (Lower Cretaceous) of the Isle of Wight, southern England. *Proceedings of the Geologists' Association, 109*, 81–91.

Rollin, K. E. (1995). A simple heat-flow quality function and appraisal of heat-flow measurements and heat-flow estimates from the UK Geothermal Catalogue. *Tectonophysics, 244*, 185–196.

Romero-Guerrero, L., Moreno-Tovar, R., Arenas-Flores, A., Marmolejo Santillán, Y., & Pérez-Moreno, F. (2018). Chemical, mineralogical, and refractory characterization of Kaolin in the regions of huayacocotla-alumbres, Mexico. *Advances in Materials Science and Engineering, 2018*, 1–11.

Ruffell, A. H., & Batten, D. J. (1990). The Barremian-Aptian arid phase in western Europe. *Palaeogeography, Palaeoclimatology, Palaeoecology, 80*, 197–212.

Ruffell, A. H., & Rawson, P. F. (1994). Palaeoclimate control on sequence stratigraphic patterns in the late Jurassic to mid-Cretaceous, with a case study from Eastern England. *Palaeogeography, Palaeoclimatology, Palaeoecology, 110*, 43–54.

Sames, B., Cifelli, R. L., & Schudack, M. E. (2010). The nonmarine Lower Cretaceous of the North American Western Interior foreland basin: New biostratigraphic results from ostracod correlations and early mammals, and their implications for paleontology and geology of the basin—an overview. *Earth-Science Reviews, 101*, 207–224.

Selley, R. C. (1996). *Ancient sedimentary environments and their subsurface diagnosis*. Psychology Press.

Sladen, C. P., & Batten, D. J. (1984). Source-area environments of late Jurassic and early Cretaceous sediments in Southeast England. *Proceedings of the Geologists' Association, 95*, 149–163.

Stewart, D.J. (1978) The sedimentology of the Wealden Group of the Isle of Wight, Department of Geology. Portsmouth Polytechnic, United Kingdom, United Kingdom, (p. 347).

Stewart, D.J. (1981a) A field guide to the Wealden Group of the Hastings area and the Isle of Wight. In: Elliott, T. (Eds) Field guides to modern and ancient fluvial systems in Britain and Spain. International Fluvial Conference, University of Keele, (pp. 31–332).

Stewart, D. J. (1981b). A meander-belt sandstone of the Lower Cretaceous of Southern England. *Sedimentology, 28*, 1–20.

Stewart, D. J. (1983). Possible suspended-load channel deposits from the wealden group (Lower Cretaceous) of Southern England. In J. D. Collinson & J. Lewin (Eds.), *Modern and Ancient Fluvial Systems* (pp. 369–384). International Association of Sedimentologists Special Publications.

Stewart, D. J., Ruffell, A., Wach, G., & Goldring, R. (1991). Lagoonal sedimentation and fluctuating salinities in the Vectis Formation (Wealden Group, Lower Cretaceous) of the Isle of Wight, southern England. *Sedimentary Geology, 72*, 117–134.

Stoneley, R. (1982). The structural development of the Wessex Basin. *Journal of the Geological Society, 139*, 543–554.

Sweetman, S. C. (2006). A Gobiconodontid (Mammalia, Eutriconodonta) from the Early Cretaceous (Barremian) Wessex Formation of the Isle of Wight, Southern Britain. *Palaeontology, 49*, 889–897.

Sweetman, S. C., & Goodyear, M. (2020). A remarkable dropstone from the Wessex Formation (Lower Cretaceous, Barremian) of the Isle of Wight, southern England. *Proceedings of the Geologists' Association, 131*, 301–308.

Sweetman, S. C., & Insole, A. N. (2010). The plant debris beds of the Early Cretaceous (Barremian) Wessex Formation of the Isle of Wight, southern England: Their genesis and palaeontological significance. *Palaeogeography, Palaeoclimatology, Palaeoecology, 292*, 409–424.

Sweetman, S. C., & Underwood, C. J. (2006). A neoselachian shark from the non-marine Wessex Formation (Wealden Group: Early Cretaceous, Barremian) of the Isle of Wight, southern England. *Palaeontology, 49*, 457–465.

Tibert, N. E., Colin, J.-P., Kirkland, J. I., Alcalá, L., & Martín-Closas, C. (2013). Lower Cretaceous nonmarine ostracodes from an Escucha Formation dinosaur bonebed in eastern Spain. *Micropaleontology, 59*, 83–91.

Ulmer-Scholle, D. S., Scholle, P. A., Schieber, J., & Raine, R. J. (2014). A color guide to the petrography of sandstones, siltstones, shales and associated rocks. *American Association of Petroleum Geologists*. https://doi.org/10.1306/M1091304

Westaway, R., Maddy, D., & Bridgland, D. (2002). Flow in the lower continental crust as a mechanism for the Quaternary uplift of south-east England: Constraints from the Thames terrace record. *Quaternary Science Reviews, 21*, 559–603.

Zhang, X., Pease, V., Omma, J., & Benedictus, A. (2015). Provenance of Late Carboniferous to Jurassic sandstones for southern Taimyr, Arctic Russia: A comparison of heavy mineral analysis by optical and QEMSCAN methods. *Sedimentary Geology, 329*, 166–176.